

# **INFRASOUND MODELING USING SOVIET EXPLOSION DATA AND INSTRUMENT DESIGN CRITERIA FROM EXPERIMENTS AND SIMULATIONS**

Jeffry L. Stevens, David A. Adams, G. Eli Baker, Heming Xu, and John R. Murphy  
Maxwell Technologies, Systems Division

Igor Divnov and V. N. Bouchik  
Institute for the Dynamics of the Geospheres, Moscow, Russia

Sponsored by U. S. Department of Defense  
Defense Threat Reduction Agency  
Contract No. DSWA01-97-C-0129

## **ABSTRACT**

This project has two distinct parts:

1. modeling of infrasound signals from atmospheric explosions and evaluation of International Monitoring System network performance using data from historic Russian nuclear tests and other infrasound data sources; and
2. analysis of infrasound instrumentation through a program of experimentation and theoretical modeling.

The Institute for the Dynamics of the Geospheres (IDG) in Moscow, Russia, has an archive of infrasound recordings from Soviet atmospheric nuclear tests that were conducted in 1957 and 1961. IDG has digitized a total of 238 infrasound waveforms from 27 atmospheric nuclear tests. Two events were high altitude explosions at Kapoustin Yar, 12 others were at the Shagan River Test Site, and the other 13 were at Novaya Zemlya. 138 of the waveforms have measurable, unclipped signals, known instrument responses, yields, and calibrations. We have been modeling this data in two ways: first, by using the data to place constraints on infrasound scaling relations; and second, by numerical modeling of the infrasound signals. Scaling relations estimate the pressure as a function of yield and range. Several scaling relations exist in the literature, and the differences between them lead to large differences in estimates of the detection threshold of the International Monitoring System (IMS). We find that a scaling relation developed by Los Alamos is most consistent with the data set. We are modeling the waveforms using modal superposition and finite difference calculations, and are also using the Infrimap package developed by BBN.

IMS network detection capability is predicted using the network simulation programs NetSim and XNICE. NetSim uses joint probabilities together with a scaling relation to calculate the detection threshold. XNICE has the additional capability of estimating the detection threshold for non-Gaussian noise distributions. We find that IMS noise levels have a distribution that is non-Gaussian and time-dependent. The noise is characterized by a fairly well-defined minimum level, but highly variable maxima. The two-station 90% probability IMS detection threshold is found to be about one kiloton with higher thresholds in ocean regions and lower thresholds on land.

A typical infrasound recording instrument uses an array of pipes connected to a central manifold to spatially filter random pressure fluctuations along the ground and so enhance the signal-to-noise ratio (S/N). We present a rapid, accurate, method of estimating the performance of any pipe configuration used for infrasound recording. We first describe experimental work that provides the physical basis for simulations and permits estimation of parameter values. We then describe the propagator method used for the calculations. The performance of a pipe array depends on the character of the noise, and so meaningful modeling of infrasound pipe array performance hinges on accurate knowledge of the temporal and spatial distribution of pressure fluctuations over the array. We discuss the physical basis for the noise model, and limitations imposed by necessary simplifications. We present the amplitude and phase responses, and their sensitivities to different parameters, of two different types of pipes used to construct the arrays: closed-ended pipes with acoustic inlets along their lengths versus open ended, otherwise impermeable pipes. Finally, we simulate the S/N enhancement for six different pipe configurations, and discuss the results' implications for instrument design.

## OBJECTIVE

The objective of this project is to develop a better understanding of infrasound excitation, propagation, and recording in order to be able to predict the capability of the IMS network to detect and identify atmospheric explosions. To accomplish this, we are gathering a data set of infrasound recordings from historical Soviet explosions, modeling these data and using them to develop improved scaling and attenuation relations. In addition, we are using experimental and numerical methods to model the response of infrasound recording instrumentation.

## RESEARCH ACCOMPLISHED

### **Part 1: Infrasound scaling and attenuation relations and IMS detection capability**

The International Monitoring System (IMS) required by the Comprehensive Nuclear Test Ban Treaty (CTBT) will include sixty infrasound stations designed to detect atmospheric nuclear explosions. A design goal is that the system be able to detect and locate explosions as small as one kiloton anywhere in the world. In order to estimate the capability of the infrasound network, it is necessary to be able to predict the amplitude of an infrasound signal at any location, and to evaluate whether the signal would be detectable above noise levels at the recording stations. Scaling and attenuation relations are empirical and/or theoretical equations that relate the amplitude and period of infrasound signals to the explosion yield and source to receiver distance. Several different relations have been developed based on theoretical infrasound modeling, and on recordings of atmospheric nuclear and chemical explosions. The different scaling relations, however, imply very different detection threshold levels. In last year's report, we discussed several scaling relations and showed that some were unrealistic, and that two scaling relations developed by Whitaker (1995) and Clauter and Blandford (1998) were consistent with the data. These scaling relations are given by the expressions:

$$\log P = 0.92 + 0.5 \log W - 1.47 \log \Delta \quad \text{AFTAC (Clauter and Blandford, 1998)} \quad (1)$$

$$\log P_c = 3.37 + 0.68 \log W - 1.36 \log R \quad \text{LANL (Whitaker, 1995)} \quad (2)$$

where  $W$  is the explosion yield in kilotons,  $\Delta$  is distance in degrees,  $R$  is distance in kilometers,  $P$  is pressure in Pascals and  $P_c$  is wind corrected pressure given by  $P_c = 10^{-0.19V}$  where  $V$  is the component of the stratospheric wind velocity in meters/second in the direction of wave motion.

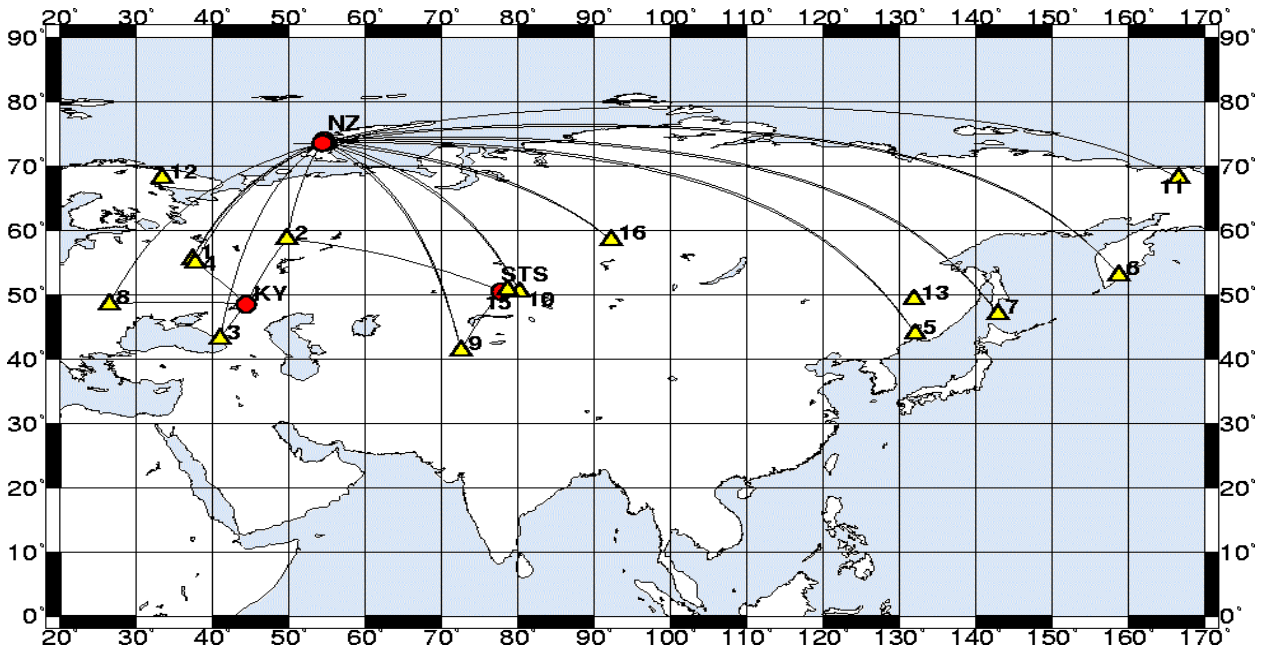


Figure 1. Stations recording infrasound signals from atmospheric explosions at three Soviet nuclear test sites Semipalatinsk (STS), Kapoustin Yar (KY), and Novaya Zemlya (NZ).

SOVIET INFRASOUND DATA

We now have a much more extensive data set of infrasound records from Soviet atmospheric explosions. IDG has an archive of approximately 300 recordings from 34 Soviet atmospheric nuclear tests that were conducted in 1957 and 1961. 20 of these explosions were located at the Novaya Zemlya test site, 12 at Semipalatinsk, and 2 at Kapoustin Yar (see Figure 1). Of these, 233 recordings from 27 of the tests recorded at stations from 1000 to 5000 km were found to be of adequate quality for digitization. The yields of these tests range from 0.4 KT to 58 MT. The data set includes two high altitude explosions and the largest (58 megaton) atmospheric explosion ever detonated. The explosions corresponding to this data set are listed in Table 1. The number of records listed in the table is the total number of records digitized for each event.

Test Site	Explosion Number	Date	Time (Moscow)	Latitude	Longitude	Height of Burst (m)	Yield (KT)	Number Records
STS	088	1961/09/04	08:00:27	50.45	77.74	725	9	2
STS	089	1961/09/05	09:00:05	50.45	77.74	500	16	3
KY	091	1961/09/06		48.45	44.30	22700	11	6
STS	094	1961/09/10				390	12	2
NZ	095	1961/09/10	12:00:14	73.52	54.30	2000	2700	23
NZ	099	1961/09/12	13:08:00	73.52	54.30	1190	1150	23
STS	100	1961/09/13	08:01:55.8	50.45	77.75	710	14	1
NZ	102	1961/09/14	12:56:16	73.52	54.3	1700	1200	17
STS	103	1961/09/14	08:59:59.4	50.35	77.82	0.5	0.4	1
STS	105	1961/09/17	10:00:46.6	50.45	77.75	695	21	1
NZ	111	1961/09/20	11:12:12	73.52	54.30	1600	2000	6
STS	112	1961/09/21	17:01:01.6	50.33	77.70	110	0.8	2
NZ	113	1961/09/22	11:11:00	73.52	54.30	1300	260	4
STS	114	1961/09/26	10:01:19.8	50.45	77.75	665	1.2	2
NZ	116	1961/10/02	13:30:50	73.92	54.55	1500	250	13
STS	117	1961/10/04	10:01:19.9	50.44	77.76	605	13	1
NZ	118	1961/10/04	10:30:55	73.52	54.30	2100	3000	13
KY	119	1961/10/06		48.45	44.30	41300	40	4
NZ	120	1961/10/06	10:00:08	73.52	54.30	2700	4000	20
STS	122	1961/10/12	08:31:03.6	50.45	77.75	670	15	1
STS	123	1961/10/17	10:00:00.8	50.45	77.75	505	6.6	2
STS	124	1961/10/19	08:30:42.6	50.45	77.73	710	10	2
NZ	125	1961/10/20	11:07:03	73.52	54.30		1450	17
NZ	126	1961/10/23	11:31:22	73.5	54.3	3500	12500	21
NZ	128	1961/10/25	11:31:05	73.52	54.3	1450	300	10
NZ	133	1961/10/30	11:33:27	73.52	54.30	4000	58000	21
NZ	147	1961/11/04	10:20:23	73.5	54.3	1750	150-1500	20

**Table 1. Soviet atmospheric nuclear explosions and the number of records for each event that have been digitized by IDG. STS is the Semipalatinsk test site, KY is Kapoustin Yar, and NZ is Novaya Zemlya.**

Seventeen stations recorded data from these tests. Figure 1 shows the paths from each event to each station in the data set. Data were recorded on instruments with varying low and high pass filters. IDG has put considerable effort into identifying the instrument parameters that were in use at each of the recording stations. Some information about the data is not available. Absolute times are not known for any of the waveforms. For two of the stations, the source to receiver distance is known, but only the general area is known for the station location.

#### Measurement of Russian data

All of the Russian data were carefully measured in a consistent manner. The data were first filtered to remove long and short period noise outside the frequency band of the data. A Butterworth filter was used with corner frequencies of .01 and .2 Hz for events with yield less than 100 kilotons, .002 and .1 Hz for events with yields between 100 kilotons and 2 megatons, and .001 and .1 Hz for events with yield greater than 2 megatons. The

amplitude and period were measured as half the maximum peak to peak amplitude and twice the time difference between the peak and trough, respectively. Measurements were made on both the acoustic wave and the low frequency Lamb wave if possible. Only data with known instrument responses were measured, and a digital correction for the instrument response was made at the observed period. A few signals with apparent calibration errors were not used. The final result is that measurements were made on a total of 133 waveforms. 107 acoustic waves from 17 events and 96 Lamb waves from 9 events were measured.

Figure 2 shows a comparison between pressure measurements made from the Russian data and equations 1 and 2. All pressures are zero to peak amplitudes in Pascals. Also shown on the figure are measurements from the US Project Dominic tests. The AFTAC relation (equation 1) fits the lower yield data quite well. The LANL relation (equation 2) appears to fit the data very well over the entire scaled range, although there is considerable scatter about the line. The pressure measurements have not been wind corrected since we have only limited information about wind conditions at the time of the tests. The data are consistent with the slopes of 0.5-0.68 of the AFTAC and LANL relations, with the LANL relation fitting the data over the widest range.

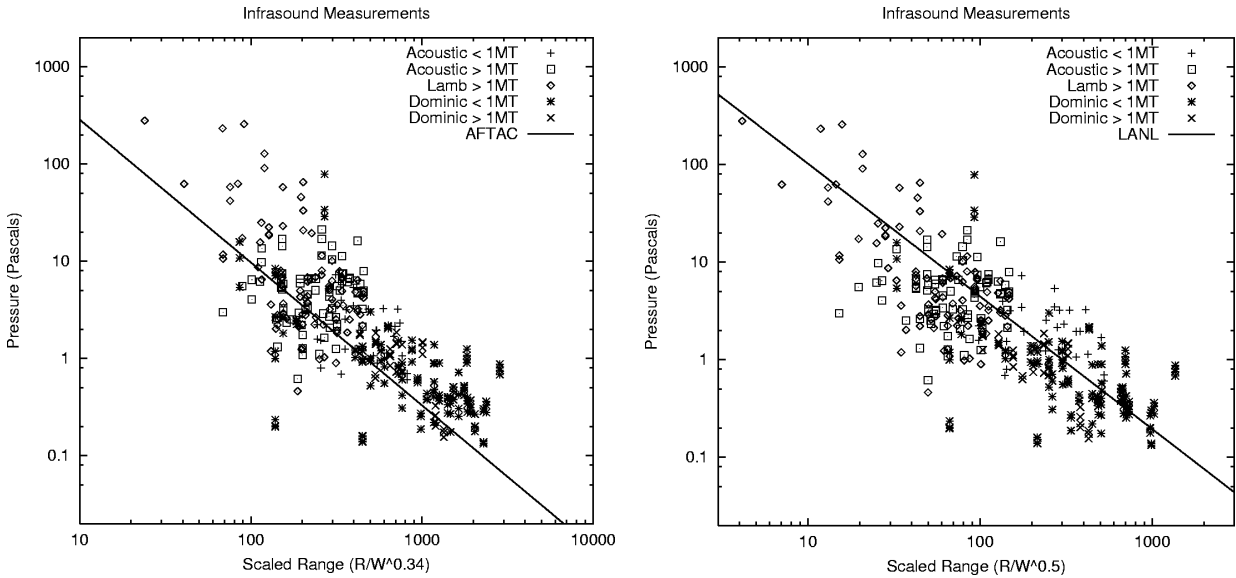


**Figure 2. Comparison of Russian data with scaling relations. Left is the AFTAC relation (Clauter and Blandford) equation 1, and right is the LANL relation (Whitaker) equation 2.**

### Infrasound Magnitudes

In the analysis above, we used a data set of infrasound waveforms from Soviet atmospheric tests ranging in yield from 6 kilotons to 58 megatons to place constraints on infrasound scaling relations and to estimate the detection threshold of the future International Monitoring System. Analysis of 133 waveforms shows that measured pressures are consistent with yield and attenuation scaling relations developed at LANL for HE tests, and also fairly consistent with a scaling relation developed by AFTAC. Because the LANL relation is consistent with data over a very wide yield range, it has recently been adopted as the basis for an infrasound magnitude by the International Data Center (IDC) (Brown, 1999). A magnitude is a useful quantity for giving an estimate of source size that is independent of the distance at which the signal is measured. The magnitude equation is:

$$M_I = \log_{10} P + 1.36 \log_{10} R - 0.019v \quad (3)$$

where the last term corrects for wind as discussed earlier. Infrasound magnitudes for the Russian data set (without wind correction), are listed in Table 2. Magnitudes for the acoustic wave and Lamb wave are listed separately. Figure 3 shows  $M_I$  plotted vs. Yield for the seven Soviet explosions. Also shown is the LANL relation, equation 2, rewritten as a magnitude/yield relation:

$$M_I = 0.68 \log W + 3.37 \quad (4)$$

As can be seen in Figure 3, equation 4 fits the data over this very wide yield range very well. An exception is the low yield, high altitude explosion at Kapoustin Yar which lies above the curve by about 0.5 magnitude units.

Test Site	Explosion	$M_I$ Acoustic	$\sigma(M_I)$ Acoustic	Number Acoustic	$M_I$ Lamb	$\sigma(M_I)$ Lamb	Number Lamb
STS	088	4.44		1			
STS	089	4.31	0.05	3			
KY	091	4.53	0.18	5			
NZ	095	5.52	0.26	16	5.50	0.25	16
NZ	099	5.29	0.46	18	5.26	0.37	20
NZ	102	5.29	0.34	13	5.13	0.31	9
NZ	111	5.56	0.40	5	5.42	0.13	3
NZ	113	4.94	0.37	2			
NZ	116	4.98	0.32	6			
STS	117	4.52		1			
KY	119	4.45	0.48	4			
NZ	120	5.38	0.48	11	5.36	0.53	12
STS	123	4.46		1			
STS	124	4.47	0.40	2			
NZ	125	5.43	0.56	9	5.24	0.41	10
NZ	126	5.33	0.35	4	6.15	0.43	14
NZ	128	5.04	0.38	6	4.92	0.38	2
NZ	133				6.69	0.40	10

**Table 2. Infrasound magnitude for eighteen Soviet explosions.**

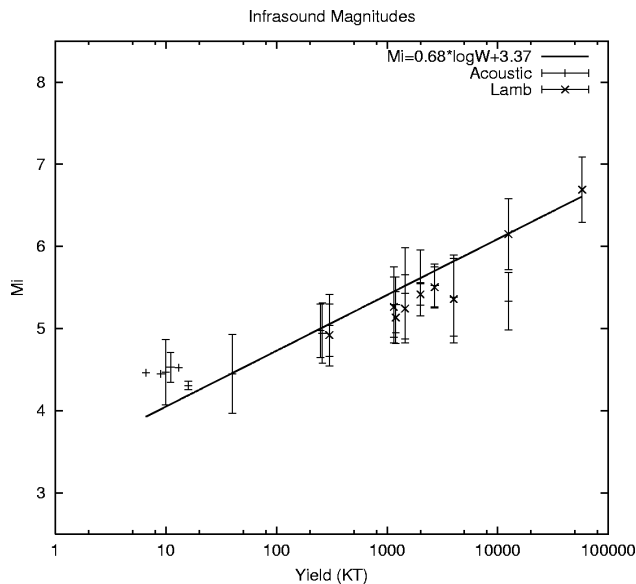


**Figure 3. Infrasound magnitude plotted vs. yield for eighteen Soviet explosions.**

### Network Detection Simulations

In order to predict the performance of the proposed 60 station IMS infrasound network, we modified the network simulation program NetSim (Serenio et al., 1990) to include the models of infrasound propagation described in equations 1 and 2. NetSim uses these equations to calculate the pressures as a function of yield

and range. These are used together with station locations, a noise model, a minimum signal to noise ratio for reliable measurement, and the number of stations required for a signal to be reported, to determine the network detection threshold as a function of position on the earth. We have calculated detection thresholds for the proposed IMS network using station dependent noise level estimates. The calculations were performed using the following parameters:

1. We used noise estimates from Blandford, et al (1995), which are based on wind measurements. The log noise levels varied from  $-1.37$  to  $-0.09$  (Pascals), with the highest levels being in oceanic regions. Log standard deviation was again taken to be 0.37.
2. The minimum signal to noise ratio for detection is 2.
3. Two stations detect infrasound signals at a 90% confidence level.
4. Four element infrasound arrays increase signal to noise ratio by a factor of 2.
5. Propagation error has a log standard deviation in log signal of 0.3.
6. Station reliability is 95%.

Detection threshold maps were calculated for the AFTAC and LANL scaling relations. The results are shown in Figures 4 and 5. For the LANL model (Figure 4), the detection threshold is between 0.5 and 2 KT. For the AFTAC model (Figure 5), the detection threshold ranges from about 0.2 KT to about 1 KT. These scaling relations predict, therefore, that the infrasound detection threshold for the IMS network is less than the design goal of one kiloton in most locations, but higher in some regions, particularly in broad ocean areas.

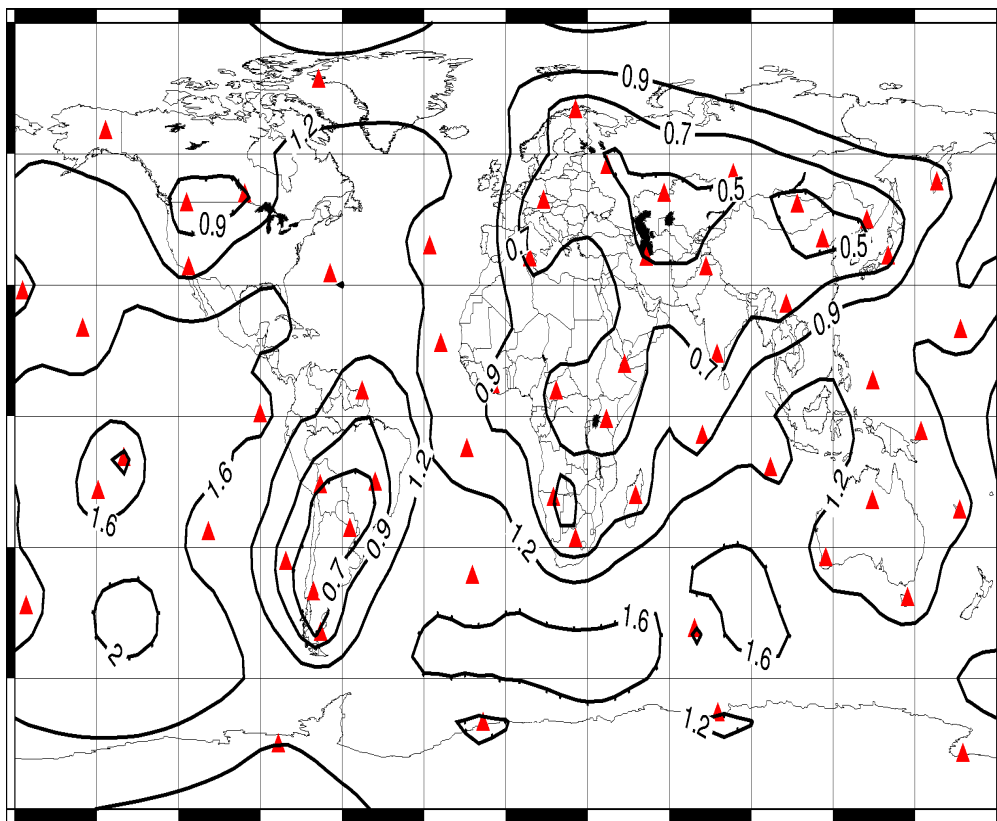


**Figure 4. Contours showing detection thresholds with a 90% level of confidence for detection at 2 infrasound stations with station dependent noise levels using the LANL scaling relation (equation 2). The intervals are logarithmically spaced with labels in kilotons.**

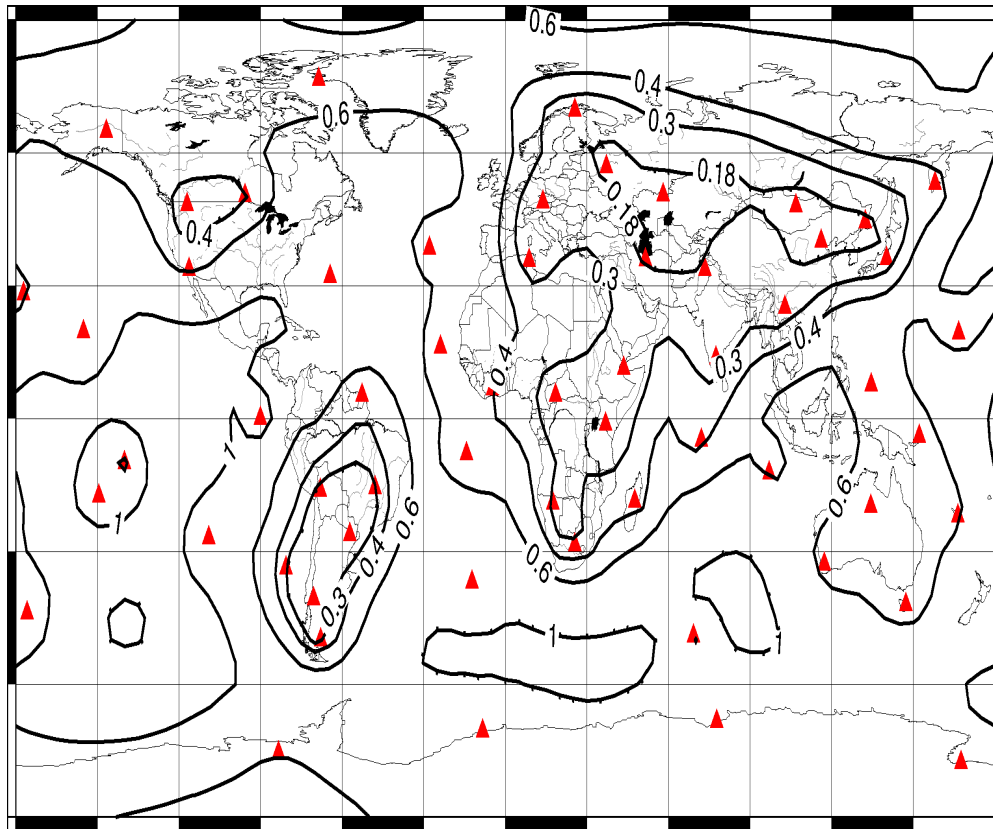


**Figure 5. Contours showing detection thresholds with a 90% level of confidence for detection at 2 infrasound stations with station dependent noise levels using the AFTAC scaling relation (equation 1). The intervals are logarithmically spaced with labels in kilotons.**

The network simulation results indicate that the detection threshold of the future IMS infrasound network may be somewhat higher than the one-kiloton design goal in some locations. This result depends, of course, on a number of assumptions that went into the simulations. We made the assumptions that a four element array leads to a factor of two improvement in signal/noise ratio, that the noise levels at all stations are independent, and that a signal will be identified with a signal to noise ratio of 2. In general, these assumptions are optimistic, although experienced analysts may be able to detect a signal at lower S/N ratios. Improvements could also be made in the signal and noise modeling. Two improvements in particular which would make the simulations more realistic are:

1. including stratospheric winds, which would have the effect of improving detection in some directions and degrading it in others.
2. Including actual noise distributions at each station instead of an average with a Gaussian distribution.

Figure 6, for example, shows the measured noise levels as a function of time over a seven month period since the start of 1999 as a time series and as a frequency distribution. Clearly the noise distribution is skewed, and much higher than average noise levels are common.

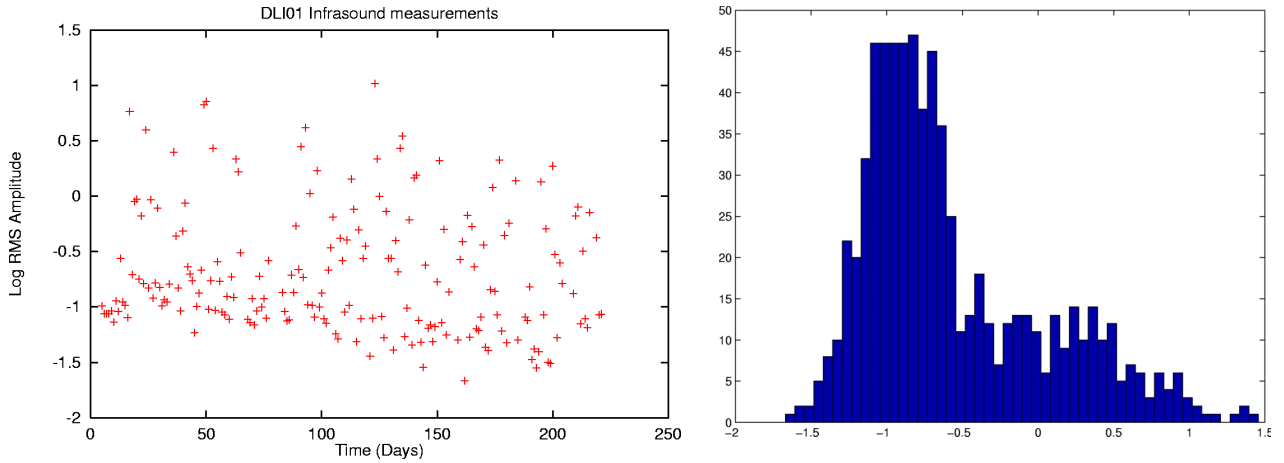


**Figure 6.** Noise measurements at the Los Alamos infrasound station since January, 1999. The left figure shows the logarithm of the RMS noise amplitude taken at noon each day since the beginning of 1999. The right figure shows the frequency distribution of the noise measurements. The distribution of noise is both skewed and time dependent.

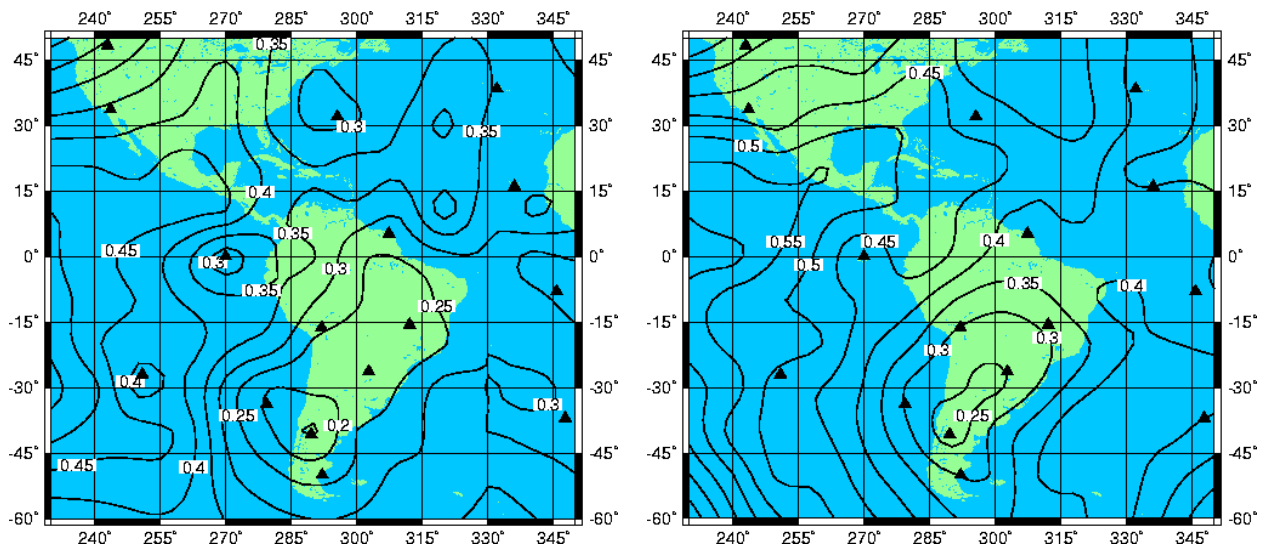


**Figure 7:** Threshold contours of yield in kilotons for 90% detection at 2 or more stations for the Gaussian noise model (left) and for the non-Gaussian noise model (right). Simulations were performed with XNICE.

NetSim does not have the capability to model non-Gaussian distributions, but they can be modeled with XNICE (Barker, 1996; Barker et al, 1994) (XNICE stands for the X Window version of the Network Identification Capability Estimation system, which can model network identification as well as detection capability). We modified XNICE to handle infrasound as well as seismic data, and did a test case to assess the difference caused by a realistic noise distribution such as that shown in Figure 6. We used a constant mean noise level at all stations of 0.1 Pascals and a minimum S/N of 1.5, and performed two test cases: one with a Gaussian distribution with a standard deviation of 0.64 (derived from the distribution in Figure 6), and one with the noise distribution modified to have the same shape as the distribution in Figure 6 at all stations. Figures 7 and 8 show the results for South America. The absolute numbers are lower than was shown in Figure 3 because the parameters used in the calculation, particularly the lower minimum S/N, are different. However, the effect of including the actual noise distribution is to increase the threshold level by about 50%,



which is a significant difference. The IMS thresholds should be reevaluated as actual noise data becomes available for the IMS infrasound stations.

### Simulations of Pipe Array Amplitude and Phase Response and S/N Improvement

We have developed a numerical model with a sound physical basis, and used it to simulate the response of arrays of pipes used as spatial filters in recording infrasonic signals. We reported (Stevens et al, 1999) on experiments to determine the physical basis for the model and to provide empirical measures of dispersion and attenuation, and on the numerical method used to simulate the amplitude and phase response of any configuration. Here we present results of simulations for various pipe configurations (Figure 8), including amplitude and phase responses (Figures 9 and 10) of open and closed ended pipe arrays, and S/N improvement under various noise conditions (Figure 11).

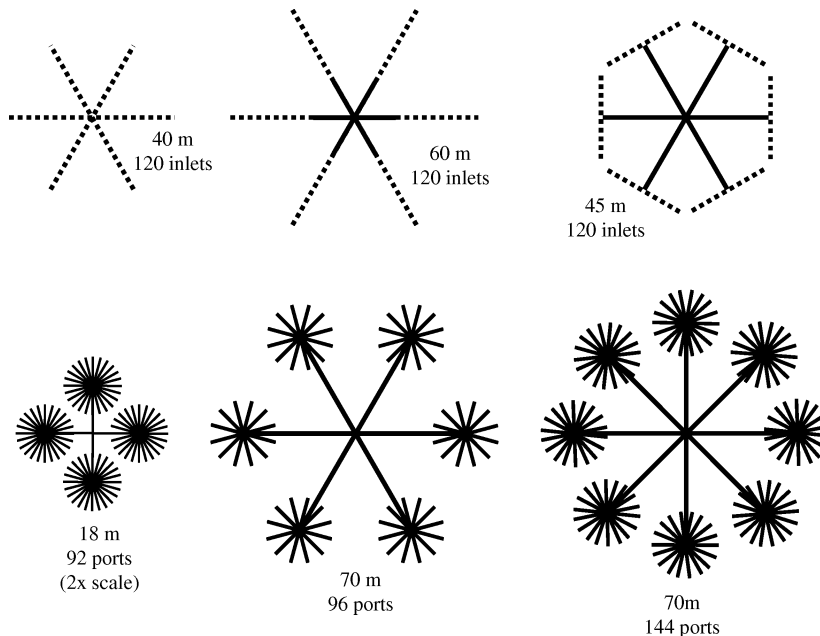


**Figure 8.** Designs for which we perform simulations (from Noel and Whitaker, 1991; Christie, 1999; Alcoverro, 1998). Close-ended arrays (top row) use 2.5 cm radius pipes with 100 acoustic ohm inlets every meter (dotted lines) connected to impermeable pipe (solid lines). Pressure is measured at a summing manifold at the center of each configuration. The long radial arms of the open-ended impermeable pipe arrays (bottom row) are 0.95 cm radius, and the shorter arms (and all pipes in the 18 m diameter configuration) are 0.64 cm radius. Summing manifolds are at the center of each set of radial arms, which are then connected by the long radial pipes to a central summing manifold where the pressure is measured.

The signal-to-noise improvement of a pipe array depends on the character of the noise, as well as on the spatial configuration. We assume that noise is due to slowly evolving eddies, with a zeroth order Von Karman distribution, advected past the instrument at the mean wind speed. We perform simulations for wind speeds of 1 and 6 m/s, and correlation lengths of 1 and 10 m (Figure 11).

We conclude that open-ended pipes hold most of the advantages over closed-ended pipes with high impedance acoustic inlets, as they have essentially flat amplitude responses while the closed-ended pipes act as lowpass filters. The open-ended pipes also have flat phase responses. The phase response of the closed-ended pipes varies much more across the spectrum of interest. The most important design criterion for enhancing S/N is sufficient spatial sampling. Extra ports spaced at less distance than the noise correlation length provide no advantage. Differences in performance are very significant at lower frequencies, with the two 70 m diameter configurations providing the best S/N enhancement. Their performances were nearly identical even though one had 144 ports and the other had only 96. The 18 m diameter configuration performed the worst at low frequency.

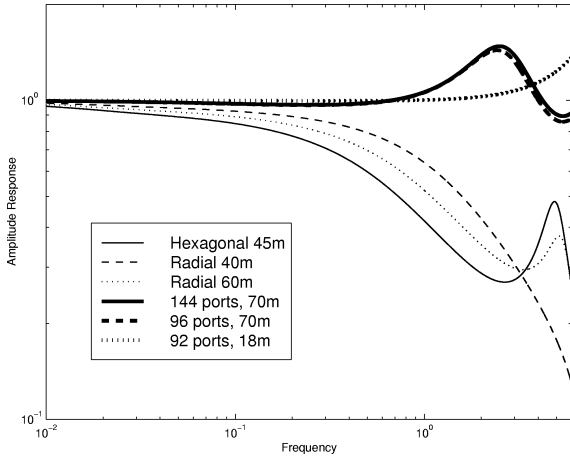


**Figure 9. Amplitude responses of configurations shown in Figure 8. Open-ended pipes provide a flat response but lower resonance frequency. In the closed-ended pipe arrays, narrower pipes could provide a somewhat flatter response.**

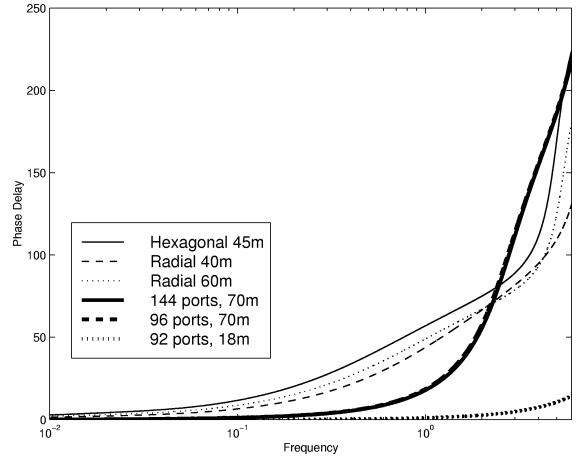


**Figure 10. Phase responses of configurations shown in Figure 8. Up to resonance frequency, the open-ended pipe arrays responses are flatter. Wider pipes would produce a flatter phase response for the close-ended pipes.**

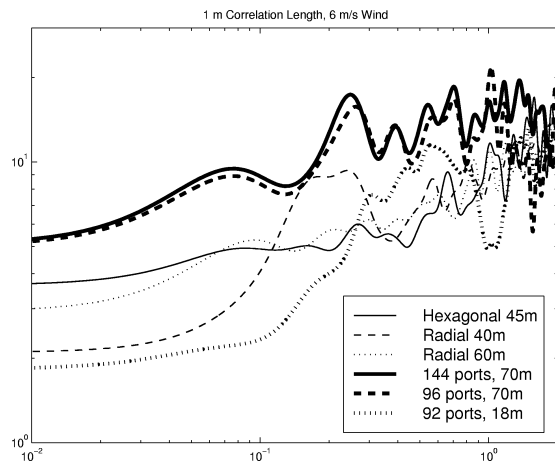
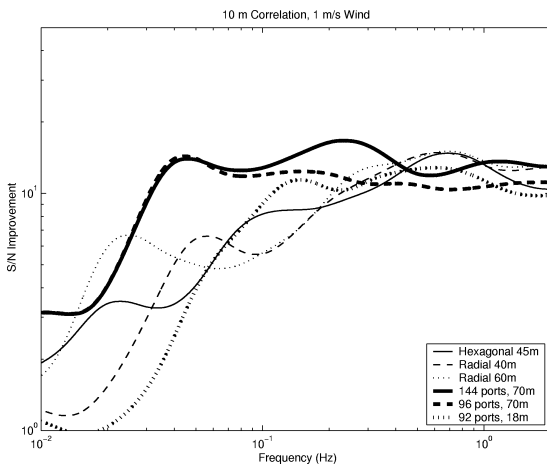


**Figure 11. S/N improvement for six different configurations (Figure 8), for 10 m correlation length self-similar noise carried past the instruments by 1 m/s wind (left) and 1 m correlation length noise advected by 6 m/s wind (right). Maximum radius spanned and number of ports (for open-ended pipes) are listed. Each of the close-ended pipe configurations has 120 inlets.**

## **CONCLUSIONS AND RECOMMENDATIONS**

In the analysis above, we used a data set of infrasound waveforms from 27 Soviet atmospheric tests to place constraints on infrasound scaling relations and to estimate the detection threshold of the future International Monitoring System. Analysis of 138 waveforms shows that measured pressures are consistent with yield and attenuation scaling relations developed at LANL for HE tests, and also fairly consistent with a scaling relation developed by AFTAC. The network simulation results indicate that the detection threshold of the future IMS infrasound network may be somewhat higher than the one-kiloton design goal in some locations, particularly in broad ocean regions. Measured infrasound noise distributions are found to be skewed and inconsistent with a Gaussian distribution. Infrasound noise measurements should be made at each IMS station location and the detection thresholds reevaluated using actual noise distributions.

We have developed a rapid, accurate, method of estimating the performance of any pipe configuration used for infrasound recording, and used it to model the response of instrument configurations being considered for the IMS infrasound network. The method is based on appropriate physics, the computations are based on propagator matrices, and results match experimental data. This will permit numerical simulation-based optimization of new designs before deployment, speeding up development and testing of new designs. It will also enable optimization of configurations where noise conditions are well known, and estimation of response curves for existing instruments. The most important step that can be taken next to improve instrument performance is to obtain, and utilize in such modeling, more complete and accurate noise models.

### **Acknowledgement**

We thank Bob Blandford and Dean Clauter for helpful discussions and for providing the station dependent noise estimates.

**Key Words:** infrasound, scaling relation, attenuation, atmospheric explosion, instrument

### **REFERENCES**

- Alcoverro, B. (1998), Acoustic filters design and experimental results, *Proceeding: Workshop on Infrasound*, Commissariat à l'Énergie Atomique, Bruyères le Châtel, France
- Barker, T.G. (1996), "Xnice: A System for Assessing Network Identification Performance," Maxwell Laboratories Scientific Report to Phillips Laboratory, PL-TR-96-2087.
- Barker, T. G., K. L. McLaughlin, and J. L. Stevens (1994), "Network Identification Capability Evaluation (NICE)", S-CUBED Technical Report to the Advanced Research Projects Agency SSS-TR-94-14701, July.
- Blandford, R. R., D. A. Clauter, R. W. Whitaker, and T. Armstrong (1995), "Infrasound Network Options," AFTAC/DOE White Paper.
- Brown, D. J. (1999) "Summary of Infrasound Source Location Meeting: San Diego, November 9-10, 1998, Center for Monitoring Research Technical Report CMR-99/02, January.
- Christie, D.R. (1999), Wind-noise reducing pipe arrays, memo of the Provisional Technical Secretariat, CTBTO, Vienna, Austria
- Clauter, D. A. and R. R. Blandford (1998), "Capability Modeling of the Proposed International Monitoring System 60-Station Infrasonic Network," proceedings of the Infrasound workshop for CTBT monitoring, Santa Fe, New Mexico, August 25-28, 1997, LANL report number LA-UR-98-56.
- Kaimal, J.C. and J.J. Finnigan (1994), Atmospheric Boundary Layer Flows: Their Structure and Measurement, Oxford Univ. Press
- Noel, S.D. and Whitaker, R.W. (1991), Comparison of noise reduction systems, LANL report LA-12008-MS UC-700
- Serenio, T. J., S. R. Bratt, and G. Yee (1990), "NetSim: A computer program for simulating detection and location capability of regional seismic networks," SAIC Annual Technical Report to DARPA, SAIC 90/1163, March.
- Stevens, J.L., D. Adams, G.E. Baker, H. Xu, J. Morris, I. Divnov, V. Bouchik, and I. Kitov, (1999), Infrasound scaling and sttenuation relations from Soviet explosion data and instrument design criteria from experiments and simulations, *Proceedings 21<sup>th</sup> Annual Seismic Research Symposium on monitoring a CTBT*, 185-194
- Whitaker, R. W. (1995), "Infrasonic Monitoring," proceedings of the 17<sup>th</sup> annual Seismic Research Symposium in Scottsdale, AZ, September 12-15, 1995, 997-1000.